



Final Draft of the original manuscript

Adyasari, D.; Waska, H.; Daehnke, K.; Oehler, T.; Pracoyo, A.; Putra, D.; Moosdorf, N.:

Terrestrial Nutrients and Dissolved Organic Matter Input to the Coral Reef Ecosystem via Submarine Springs.

In: ACS ES & T Water. Vol. 1 (2021) 8, 1887 – 1900.

First published online by ACS: 29.07.2021

<https://dx.doi.org/10.1021/acsestwater.1c00134>

1 **Terrestrial nutrients and dissolved organic matter input to the coral reef ecosystem via**
2 **submarine springs**

3
4 Dini Adyasari^{a,b*}, Hannelore Waska^c, Kirstin Daehnke^d, Till Oehler^a, Atas Pracoyo^e, Doni Prakasa
5 Eka Putra^f, Nils Moosdorf^{a,g}

6
7 ^aDepartment of Biogeochemistry and Geology, Leibniz Centre for Tropical Marine Research
8 (ZMT), Bremen 28359, Germany

9 ^bDepartment of Geological Sciences, University of Alabama, Tuscaloosa, AL 35487, USA

10 ^cInstitute for Chemistry and Biology of the Marine Environment (ICBM), Carl von Ossietzky
11 University of Oldenburg, Oldenburg 26129, Germany

12 ^dDepartment of Ecosystems and Biogeochemical Cycles, Helmholtz Centre for Materials and
13 Coastal Research, Geesthacht 21502, Germany

14 ^eFaculty of Engineering, Universitas Mataram, Mataram 83115, Indonesia

15 ^fDepartment of Geological Engineering, Universitas Gadjah Mada, Yogyakarta 55281, Indonesia

16 ^gInstitute of Geosciences, Christian-Albrechts-Universität zu Kiel, Kiel 24118, Germany

17
18 *Corresponding author:

19 Email: dadyasari@ua.edu

20

21 **Abstract**

22 Submarine groundwater discharge (SGD) transports terrestrial nutrients and dissolved organic
23 matter (DOM) to the ocean. Elevated concentration of nutrients and DOM can act as stressors
24 enhancing coral disease and mortality, but only a few studies address the impacts of groundwater-
25 borne nutrients and DOM on coral reef ecosystems. This study quantifies and characterizes
26 nutrients, nitrate (NO_3^-) stable isotopes, and DOM molecular composition of coastal groundwater
27 discharging to the reef ecosystem via submarine springs in Lombok, Indonesia. NO_3^- isotopic
28 values point to both natural (soil) and anthropogenic (wastewater and fertilizer) origins of nutrients
29 in the coastal aquifer. Submarine springs are fed by different groundwater sources and deliver
30 land-based NO_3^- , dissolved silica, phosphate, and labile DOM to the reef water column. Terrestrial
31 nutrients and DOM undergo rapid turnover in the reef water column due to biogeochemical
32 processes and biological uptake. Meanwhile, reef and offshore water likely act as sources of more
33 stable, reworked DOM formulae and its mineralization product, ammonium. We observed that
34 submarine springs consistently deliver similar nutrient loadings, creating a long-term
35 environmental threat to coral reef sustainability. This study emphasizes the importance of
36 understanding coastal biogeochemistry and hydrological processes in sensitive tropical
37 ecosystems, particularly those adjacent to modified land-use watersheds.

38

39 **Keywords**

40 Submarine groundwater discharge, nutrients, dissolved organic matter, coral reef ecosystem,
41 ultrahigh-resolution mass spectrometry, tropics, Coral Triangle.

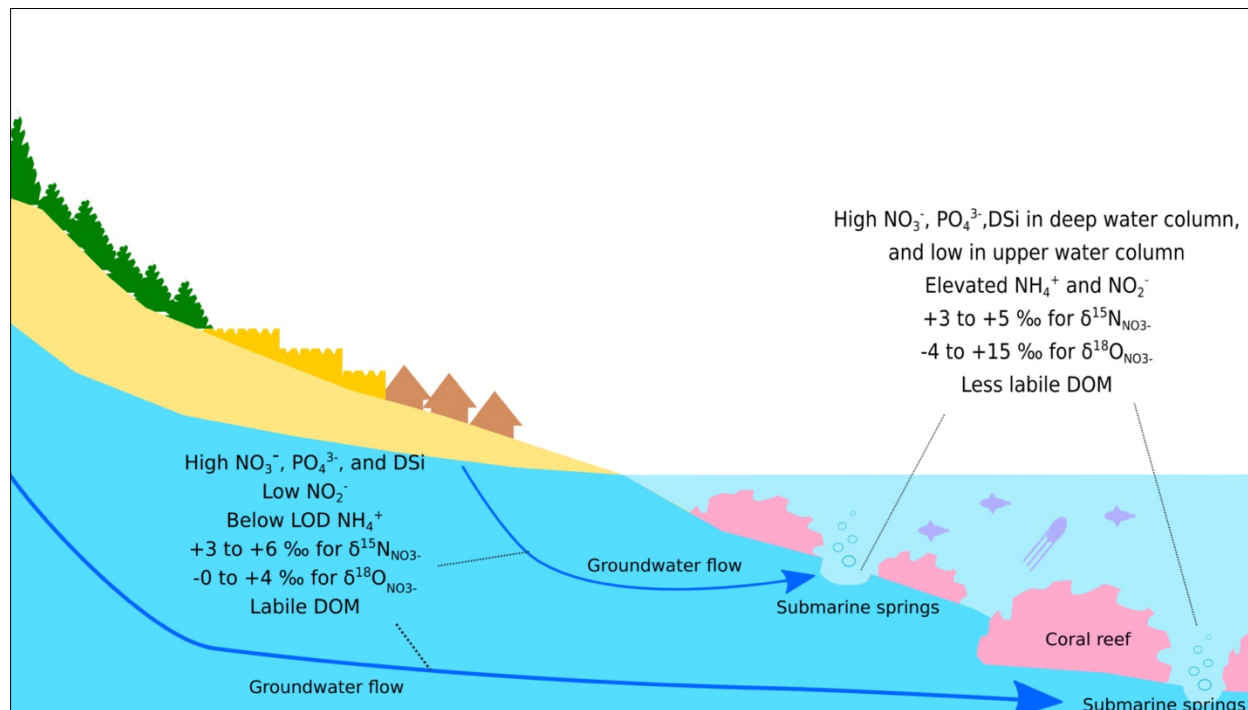
42

43 **Synopsis**

44 Understanding the source and transformation of terrestrial nutrient and organic matter transported
45 to coral reef ecosystems via submarine groundwater discharge is important to protect coral's
46 health.

47

48 **Graphic for TOC**



49

50

51 **INTRODUCTION**

52 Submarine groundwater discharge (SGD) is defined as direct groundwater outflow across the
53 land-ocean interface into the coastal ocean^{1,2}. More than 90% of total SGD is estimated to be in
54 the form of recirculated seawater or "marine SGD" at a global scale, while terrestrial or "fresh
55 SGD" does not exceed 10% of SGD volume^{3,4}. However, fresh SGD can also create ecological
56 impact in local scale. For example, as SGD is known to transport land-based nutrients⁵, heavy
57 metals⁶, organic matter (OM)⁷, or biological matter⁸, it may cause eutrophication or harmful algal
58 bloom⁹, as well as a change in phytoplankton communities or other marine biota in the receiving
59 coastal water¹⁰. In this study, we focus on fresh SGD via submarine springs. Submarine springs
60 usually occur as terrestrial groundwater conduits in a karstic or volcanic setting and may play a
61 major role in delivering land-based dissolved materials into the ocean, particularly in the tropical
62 regions^{11,12}. Southeast Asia, one of the most populated subregions in the tropics, is characterized

63 by hydrogeological and societal conditions favoring ubiquitous occurrence of, in particular, fresh
64 SGD and its associated solute fluxes: The region is characterized by heavy precipitation year-
65 round, high aquifer permeability, and fast weathering, nutrient-rich rocks¹³. In addition, Southeast
66 Asia is listed among the regions with the strongest human modifications of the coastal zone
67 worldwide¹⁴, which usually leads to increasing amounts of anthropogenic contaminants in the
68 natural water system. The region also hosts native coastal ecosystems such as coral reefs,
69 seagrass, and mangrove communities, which are sensitive to even slight increases in terrestrial
70 nutrient and OM input¹⁵.

71 The impact of the enrichment of dissolved inorganic nutrients (nitrate (NO_3^-), nitrite (NO_2^-),
72 ammonium (NH_4^+), and phosphate (PO_4^{3-})) on coral reef ecosystems has been widely studied,
73 and it is generally suggested that they negatively affect coral physiology and functioning¹⁶.
74 Previous organic matter-related studies on the coral reef ecosystem suggest that elevated
75 dissolved organic carbon (DOC) concentration can be a primary stressor resulting in coral
76 mortality^{17,18}. In recent days, DOM molecular characterization is employed to distinguish its origin
77 and distribution in this ecosystem, which may be an important step towards understanding the role
78 of DOM subsidies in reef ecosystem function^{19,20}. However, the analysis of DOM molecular
79 composition is limited due to its high complexity²¹. The recent advance of ultrahigh-resolution
80 Fourier-transform ion cyclotron resonance mass spectrometry (FT-ICR-MS) allows the
81 characterization of thousands of molecular formulae in the complex DOM mixtures from water
82 samples²². FT-ICR-MS has been implemented to study DOM characterization in different
83 hydrological settings, e.g., groundwater²³, rivers^{24,25}, subterranean estuaries (STE)^{26,27}, and
84 ocean waters of temperate^{28,29} and boreal regions²⁸, but high-resolution DOM studies from tropical
85 ecosystems are scarce. Considering that the coastal tropics of Southeast Asia are challenged with
86 elevated terrestrial nutrient and DOM export in the next years³⁰ and the adverse impact these
87 solutes may cause to the coral reef ecosystem; understanding the sources, fate, and

88 transformation of nutrients and DOM in this system is essential in predicting and managing how
89 these ecosystems will respond to global change.

90 In this study, we present physical and geochemical observations from a submarine spring complex
91 in the volcanic tropical island of Lombok, Indonesia, which discharges into a coral reef ecosystem.
92 A recent review from Indonesia shows that nutrients and organic pollutants are the two major
93 contaminants contaminating coastal water quality and ecosystems in this region, with coral reef
94 ecosystem is found as the most sensitive to terrestrial anthropogenic disturbance³¹. Therefore,
95 the objectives of this study are (1) to explore the source, fate, and transformation of nutrients in
96 the coastal groundwater, submarine springs, and water column in a coral reef ecosystem, (2) to
97 examine the previously unknown DOM molecular composition in the coastal groundwater,
98 submarine springs, and water column in a coral reef ecosystem, and (3) to evaluate the potential
99 long term environmental impact on coral reef ecosystems receiving terrestrial nutrient and DOM
100 via submarine springs.

101

102 **MATERIAL AND METHODS**

103 **Study site**

104 The submarine spring complex is located on the island of Lombok, Indonesia (Figure 1A). The
105 coral reef ecosystem in this island is a part of the Coral Triangle, a marine area across six countries
106 (Indonesia, Malaysia, Papua New Guinea, the Philippines, the Solomon Islands, and Timor-Leste)
107 which contains 76% of the world's coral species³². The land use in the island consists of natural
108 forest in the hinterland and agriculture and plantation in the coastal area (Figure 1A). Mount Rinjani
109 (3726 m a.s.l) is the highest active volcano in Lombok, situated approximately 15 km south of the
110 submarine spring complex where we conducted our study. In the northern part of the island, it can
111 be expected that about 15% of the rainwater percolates into groundwater, which is vulnerable to
112 pollution based on the local hydrogeology³³. The aquifers most likely discharge their freshwater in
113 the nearshore area below the sea as submarine springs³⁴. River discharge into the coastal water

114 in this area is located approximately 1 km towards north and south of the submarine spring
115 complex; however, these are non-perennial rivers. Several local studies have been implemented
116 at the springs, e.g., related to the springs and their identification via thermal satellite^{35,36}, the
117 potential occurrence of coral reef diseases surrounding the springs³⁷, and the utilization of the
118 springs as freshwater resources for local communities³⁸. The morphology of the springs, SGD
119 rates, and their associated nutrient fluxes were studied by Oehler, et al. ¹². In general, the springs
120 investigated in the previous works and this study are divided into three sub-complexes: Spring A,
121 Springs B-C, and Springs D-E due to their distance from each other and spring type. In the largest
122 and deepest spring in the area (Spring A), submarine groundwater discharges from an eight-
123 meter-deep structure in the form of a crater in the reef, whereas in other sites, groundwater
124 discharges from fissures and cracks in the reef (Springs B, C, D, and E) (Figure 1B).

125

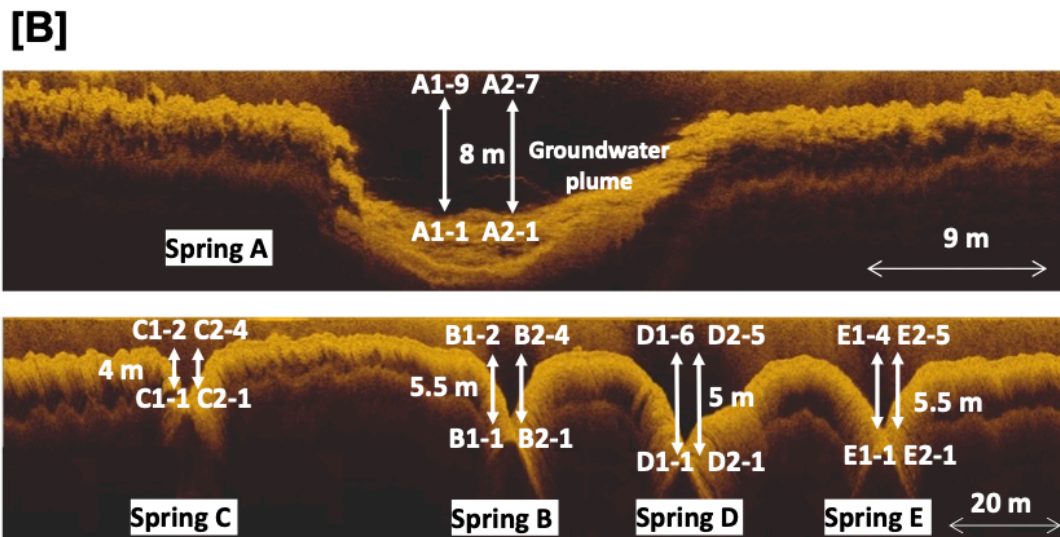
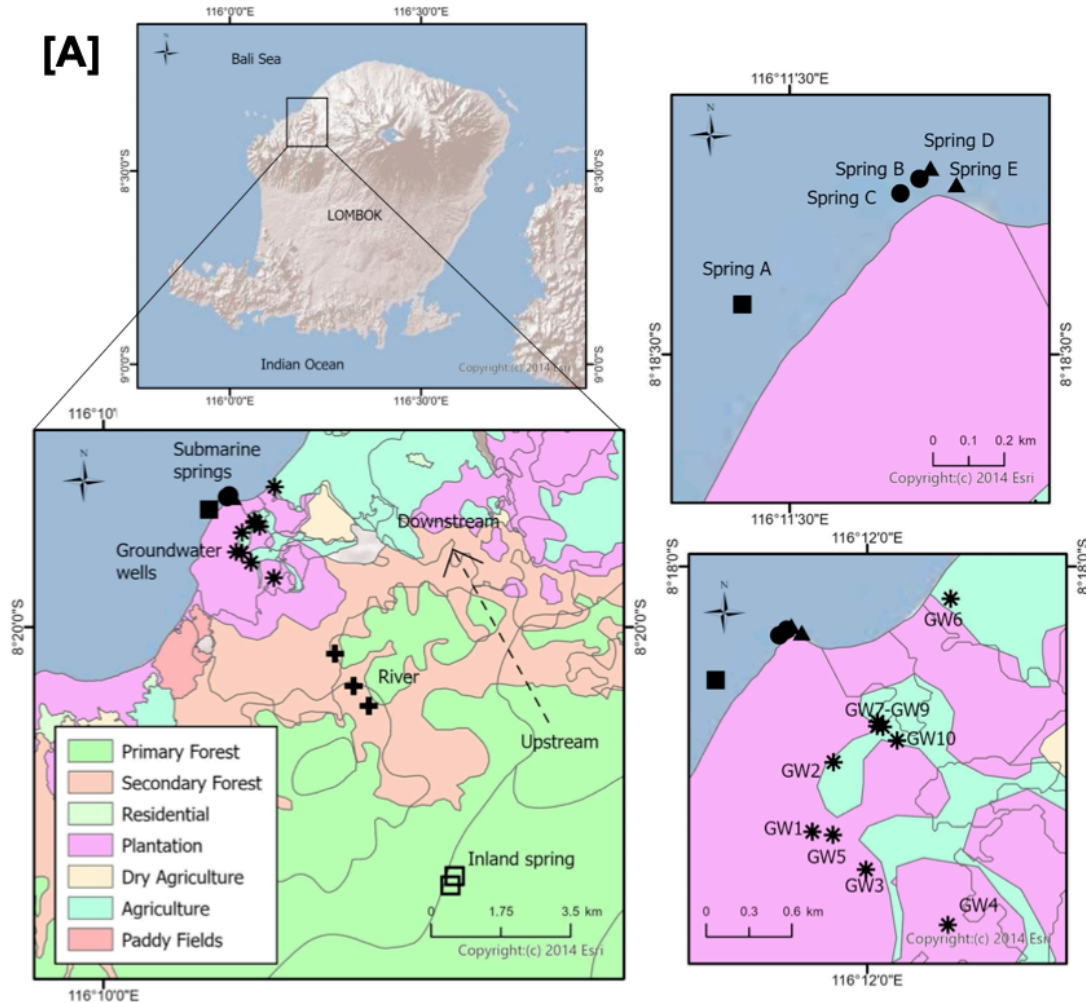


Figure 1. (A) Map of land use and sampling points in Lombok, Indonesia, and (B) vertical sampling points in the submarine springs, projected onto echosounder profiles from Oehler, et al.¹². The samples collected from December 2019 were named A1, B1, C1, D1, and E1 for submarine springs A, B, C, D, and E, respectively; while A2, B2, C2, D2, and E2 were samples from January 2020. The numbering after hyphenation indicates depth where samples were taken, where low number signify deeper depth and high number signify upper depth.

126
127
128
129
130
131
132

133 **Field sampling**

134 The field expedition was conducted in December 2019 and January 2020. Water samples were
135 collected from inland springs, rivers, groundwater wells, submarine springs, and reef water (Figure
136 1A). Two inland spring samples were collected from the northern slope of Mount Rinjani. Inland
137 spring water samples were collected by submerging the sample bottle in discharge points. River
138 samples were taken approximately 6 km to the hinterland from the coastline because they were
139 non-perennial rivers and did not discharge to the coastal area at the time of our study. River water
140 samples were collected from a depth of about 20 cm below the surface water level. Coastal
141 groundwater was sampled from ten wells owned by the local residents and consisted of three
142 shallow dug wells (depth < 3 m, i.e., GW1, GW2, GW5), and the rest of the groundwater samples
143 were taken from drilled wells (depth 12-25 m). Coastal groundwater samples were taken through
144 plastic tubing by submersible pump and the samples were collected after letting the water from
145 the well flow for a few minutes, until standing water in the surface/upper part of the well were
146 removed. Figure 1A shows the collection points from upstream to downstream, and Figure 1B
147 displays the naming of samples taken from submarine springs and their plumes. The samples
148 collected from December 2019 were named A1, B1, C1, D1, and E1 for submarine springs A, B,
149 C, D, and E, respectively; while A2, B2, C2, D2, and E2 were samples from January 2020.
150 Samples were also collected from the submarine spring plume, i.e., from discharge point to
151 surface water. Samples from discharge points were obtained from each submarine spring by
152 inserting a 2-inch diameter PVC pipe into the center of each respective spring and the water which
153 flowed through the pipe was captured in a low-density polyethylene plastic bag. The samples
154 collected from these pipes were further named A1-1, A2-1, B1-1, B2-1, C1-1, C2-1, D1-1, D2-1,
155 E1-1, and E2-1. More spring samples were collected along a vertical gradient of the submarine
156 spring plume from bottom to the surface, as seen in Figure 1B. Samples were processed on the
157 boat based on each parameter's requirement as soon as the divers reached the surface.
158 Samples from submarine springs were taken between 10.00-12.00, in the period following the low

159 tide. Water samples for seawater/ocean end member were collected approximately 1 km in the
160 offshore direction from the submarine spring complex.

161

162 **Water sample analysis**

163 Physical parameters were measured using a Hach Lange Multi 410d portable multimeter. Salinity
164 and temperature were measured with a Hach CDC401 probe, while pH and dissolved oxygen
165 (DO) were measured using Hach PHC101 and LDO101 probes, respectively. DO was measured
166 immediately after collection to prevent contamination of atmospheric oxygen. Submarine springs
167 and offshore water samples were measured immediately in the boat inside a sample bottle before
168 filtration. Water samples for nutrient analyses were filtered in the field using Whatman cellulose
169 acetate filters with a pore size of 0.45 μm and transferred into clean high-density polyethylene
170 (HDPE) vials. For nutrient measurement (NO_3^- , NO_2^- , NH_4^+ , PO_4^{3-} , dissolved silica (DSi)), the
171 samples were frozen until analysis. Nutrient analyses were conducted at the Leibniz Centre for
172 Tropical Marine Research (Germany), using a segmented flow Skalar SANplus System Instrument
173 for marine samples and a Tecan microtiter plate reader for freshwater samples. These samples
174 were measured spectrophotometrically as described by Grasshoff, et al. ³⁹. Tecan microtiter plate
175 reader has a limit of detection (LOD) of 12 μM (NO_3^-), 0.2 μM (NO_2^-), 4 μM (NH_4^+), 0.2 μM (PO_4^{3-}
176), and 1.4 μM (DSi). In this paper, dissolved inorganic nitrogen (DIN) refers to total NO_3^- , NO_2^- ,
177 and NH_4^+ .

178 Samples for nitrogen and oxygen isotopic composition of dissolved NO_3^- ($\delta^{15}\text{N}_{\text{NO}_3^-}$ and $\delta^{18}\text{O}_{\text{NO}_3^-}$)
179 were frozen until analysis at the Helmholtz Centre for Materials and Coastal Research, Germany.
180 The water samples were analyzed using the denitrifier method^{40,41}. NO_2^- was removed using
181 sulfamic acid prior to N and O isotope analysis if the samples contained NO_2^- concentrations of
182 more than 2% of the respective NO_3^- concentrations⁴². The isotopic composition was determined
183 on a GasBench II coupled to a Delta V Advantage mass spectrometer (ThermoFinnigan).
184 Replicate measurements were performed using two international standards (IAEA-N3, $\delta^{15}\text{N} =$

185 +4.7‰, $\delta^{18}\text{O} = +25.6\text{‰}$ and USGS 34 $\delta^{15}\text{N} = -1.8\text{‰}$, $\delta^{18}\text{O} = -27.9\text{‰}$ ⁴³) with each batch of samples.

186 The standard deviation of samples and standards was < 10% for $\delta^{15}\text{N}$ and 28% for $\delta^{18}\text{O}$. To correct
187 for exchange with oxygen atoms from water, a bracketing correction was applied based on
188 Sigman, et al.⁴⁴. $\delta^{15}\text{N}_{\text{NO}_3^-}$ and $\delta^{18}\text{O}_{\text{NO}_3^-}$ values are reported per mill (‰) relative to AIR and
189 VSMOW, respectively. We applied a conservative mixing calculation by Fry⁴⁵ to assess the mixing
190 pattern of groundwater and coastal NO_3^- isotopes and to detect internal sources and sinks over
191 the course of the mixing gradient.

192 Samples for DOC, DOM, and total dissolved nitrogen (TDN) were filtered with 0.22 μm
193 polyethersulfone filter, acidified with HCl to pH=2, and kept at 4°C temperature until analyzed in
194 the laboratory of the Institute for Chemistry and Biology of the Marine Environment (ICBM),
195 University of Oldenburg, Germany. DOC and TDN concentrations were measured by high-
196 temperature catalytic oxidation (HTCO) on a Shimadzu TOC-VCPH instrument equipped with a
197 TDN unit against a deep Atlantic seawater reference material (D.A. Hansell, University of Miami,
198 FL, USA). Accuracy and precision were better than 5% and 15%, respectively. DON was
199 calculated as the difference between TDN and DIN concentration. Note that this might lead to
200 uncertainties due to the use of two different analytical methods, especially when DIN
201 concentrations highly exceed DON concentrations⁴⁶. Therefore, DON results have to be
202 interpreted with caution.

203 Before DOM molecular composition analyses, the HCl-acidified samples were desalinated and
204 pre-concentrated using Agilent BOND ELUT PPL cartridges following the protocol of Dittmar, et
205 al.⁴⁷. 50 mL subsamples were extracted into a methanol matrix of ~1.2 mL volume. DOC recovery
206 was quantified in extract subsamples, dried in an oven to remove the methanol solvent and re-
207 dissolved in ultrapure water acidified to pH=2 with HCl for DOC measurement. From the remainder
208 of the DOM extracts, subsamples were diluted to a DOC concentration of 2.5 ppm in a 1:1 mixture
209 of methanol and ultrapure water. The subsamples were then measured via flow injection on a 15T
210 solariX XR FT-ICR-MS with electrospray ionization (ESI) in negative ionization mode, using a

211 HyStar Autoanalyzer. Sample mass spectra were uploaded into the online freeware ICBM-
212 OCEAN⁴⁸ to remove instrument blanks and align samples based on their masses. Based on the
213 elemental stoichiometry of assigned molecular formulae, ICBM-OCEAN groups them into the
214 categories "aromatic," "highly unsaturated," "unsaturated," and "saturated." We normalized the
215 relative abundance of each category by multiplying them with SPE-DOC concentration to
216 determine their distribution and quantities in the DOM pool. For each assigned formula, ICBM-
217 OCEAN also calculates an aromaticity index (AI_{mod}), which is indicative of the presence of
218 aromatic ring structures in the compound. H/C and O/C molar ratios were calculated to indicate
219 degrees of saturation and oxygenation⁴⁹. For all of the abovementioned characteristics, intensity-
220 weighted averages were calculated for each sample after normalizing the relative intensities of
221 each formula to the sum of intensities of the whole respective sample.

222 Furthermore, for this study, we calculated molecular indices of provenance or processing which
223 have been reported in the literature: A microbial productivity index $I_{bioprod}$ ⁵⁰, a DOM degradation
224 index I_{deg} ⁵¹, a terrestrial index I_{Terr} ⁵², and a lability index MLB_I ⁵³. $I_{bioprod}$ comprises of ten ubiquitous
225 molecular formulae associated with fresh DOM release from aquatic primary production in a
226 controlled marine mesocosm⁵⁰. I_{deg} consists of ten ubiquitous molecular formulae that were
227 developed in an open ocean setting and calibrated against the $\Delta^{14}C$ radiocarbon age of DOM⁵¹.
228 I_{Terr} consists of 80 ubiquitous molecular formulae, which were significantly correlated with the
229 salinity gradient of the Amazon estuary⁵². MLB_I index considers the H/C ratio of all molecular
230 formulae in a sample, dividing them along a "molecular lability boundary" of $H/C = 1.5$ ⁵³.

231

232 **Data analysis**

233 Figure visualization and multivariate statistical analysis for DOM composition were performed in
234 R (R version 4.0.3⁵⁴) using 'vegan' R package version 2.5-6⁵⁵. Correlation between environmental
235 parameters was analyzed using Spearman correlation, and only correlations with p-value < 0.001
236 were considered for analysis and discussion. Non-metric multidimensional scaling (NMDS) was

237 performed as an ordination method for DOM molecular composition. DOM molecular indices and
238 intensity-weighted averages of characteristics such as oxygen content, saturation, and aromaticity
239 were mapped to the NMDS plot using *envfit*. Distance based linear model (DistLM) using the
240 function *adonis2* was applied to relative abundances of assigned formulae in DOM to determine
241 which environmental variables best explained the variation in DOM molecular composition.

242

243 **RESULTS AND DISCUSSION**

244 **Biogeochemistry of coastal groundwater**

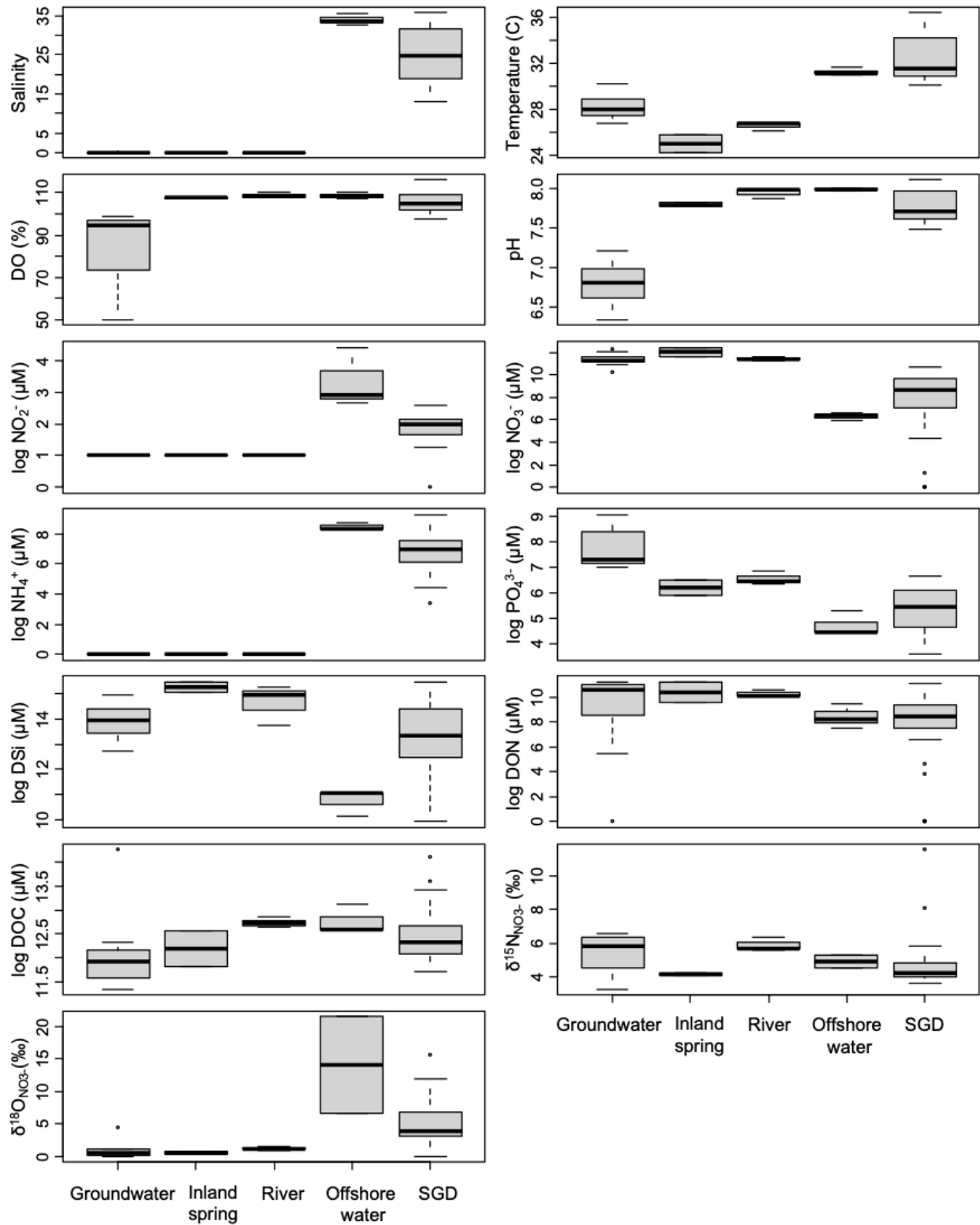
245 The range of physicochemical water parameters is displayed in Figure 2, while measurement
246 results of all samples are included in the Supplementary Material. Groundwater was characterized
247 by medium temperature (range 26 - 30 °C), low salinity (range 0.09 - 0.19), medium to oxygenated
248 condition (DO range 48 to 98%), and mildly acidic (range 6.3 - 7.2) water (Figure 2).

249

250 *Nutrients*

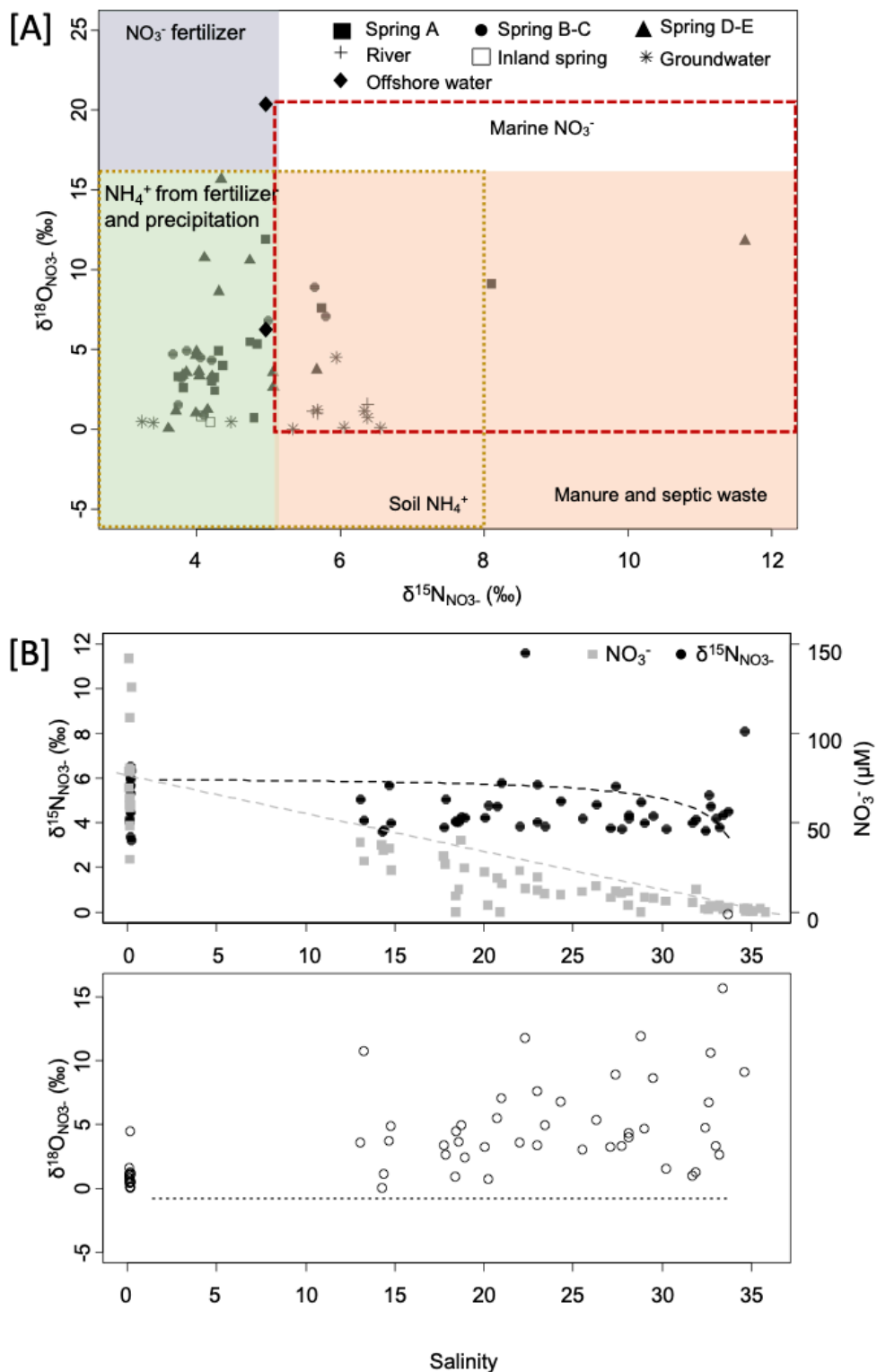
251 NO₃⁻ composed the major species of the dissolved nitrogen pool in the groundwater with a
252 concentration between 29-125 μM, followed by DON (range 0-60 μM), NO₂⁻ (range 0-0.05 μM),
253 and NH₄⁺ (< 4 μM, below LOD) (Figure 2). NO₃⁻ concentration in the inland spring located on the
254 mountain slope was slightly higher (range 78 – 142 μM, n = 2) than in the coastal groundwater
255 (range 29 – 125 μM, n = 10). The stable isotope values for groundwater were in the range of +3.24
256 to +6.56 ‰ for δ¹⁵N_{NO3-} and -0.49 to + 4.50 ‰ for δ¹⁸O_{NO3}, while the inland springs spanned a
257 narrower range (δ¹⁵N_{NO3-} range +4.06 to +4.19 ‰, δ¹⁸O_{NO3} range -0.85 to + 0.46 ‰) (Figure 2,
258 Figure 3A).

259



260

261 **Figure 2.** Concentrations of different physicochemical properties in groundwater, inland spring,
 262 river, seawater, and SGD samples. Nutrient (NO₃⁻, NO₂⁻, NH₄⁺, PO₄³⁻, DSi, DON) and DOC
 263 concentrations are given in (log x) + 1 μM.



264

265 **Figure 3.** (A) $\delta^{15}\text{N}_{\text{NO}_3^-}$ and $\delta^{18}\text{O}_{\text{NO}_3^-}$ plotted in a diagram of the isotopic composition of potential
 266 NO_3^- sources, modified from Kendall, et al. ⁵⁶. (B) NO_3^- concentration and $\delta^{15}\text{N}_{\text{NO}_3^-}$ plotted versus
 267 salinity (top), and $\delta^{18}\text{O}_{\text{NO}_3^-}$ plotted versus salinity (bottom). In both figures B, dashed lines
 268 indicate theoretical conservative mixing.

269 The NO_3^- isotope value signatures have long been employed to determine N sources in the
270 groundwater system. NO_3^- isotope values from coastal groundwater samples in this study are
271 plotted in the overlapping signatures characteristic for natural and anthropogenic activities: soil
272 NH_4^+ , manure and septic waste, or NH_4^+ in fertilizer and precipitation (Figure 3A). We ruled out
273 precipitation as the area had not received rainfall three months before the sampling activity. Soil
274 NH_4^+ was a potential source of NO_3^- even though its concentration in groundwater was below LOD,
275 considering NH_4^+ is usually immobile in soils due to adsorption and ion exchange to clay
276 particles⁵⁷.

277 The $\delta^{15}\text{N}_{\text{NO}_3^-}$ signature also pointed to possible anthropogenic sources such as septic waste,
278 manure, and fertilization. Northern Lombok only had a household sanitation coverage of roughly
279 80%⁵⁸. Approximately 20% of the household do not have access to discharge their wastewater
280 properly and might contribute to the groundwater $\delta^{15}\text{N}_{\text{NO}_3^-}$. Manure or wastewater from livestock
281 was also not regulated and could be a potential contribution. As for fertilization, the Ministry of
282 Agriculture reported that farmers in Lombok used a mixture of inorganic fertilizers, i.e., urea, ZA
283 (ammonium sulfate, 21% N and 24% S), SP-36 (superphosphate, 36% P_2O_5), and KCl (potassium
284 chloride, 60% K_2O) to fertilize their agricultural fields two times per year⁵⁹. Theoretically, urea and
285 ZA could contribute to the low isotope signature, as NO_3^- that is initially formed from these
286 fertilizers should be isotopically depleted because nitrification strongly discriminates against the
287 heavy isotope species. Overall, we could not delineate specific sources of groundwater NO_3^-
288 based on $\delta^{15}\text{N}_{\text{NO}_3^-}$ signature alone. However, the highly elevated PO_4^{3-} concentration (3.20-13.20
289 μM), which exceeded the environmental regulation limit for groundwater⁶⁰, points towards
290 anthropogenic contamination.

291 If anthropogenic sources indeed contaminate the coastal area, we expect higher groundwater
292 NO_3^- concentration in the cultivated downstream area than in the pristine upstream area. On the
293 other hand, we presume that there are other sources other than the inland springs we sampled
294 feed into the coastal aquifer. These other sources may contain low NO_3^- concentration and dilute

295 NO₃⁻ concentration in the downstream area relative to inland spring NO₃⁻ concentration. A locally
296 important contribution of additional water sources was also supported by considerable scatter on
297 the NO₃⁻ isotope data in Figure 3A. Considering the coastal land use map where the downstream
298 area consists of agriculture and plantation (Figure 1A), we propose that anthropogenic sources
299 contribute to groundwater NO₃⁻ concentration in the downstream area; however, their contributions
300 were weakened by different water input to the coastal aquifer.

301 The relatively low δ¹⁸O_{NO3-} values (< 5‰) in coastal groundwater samples suggests the occurrence
302 of nitrification, which was also supported by high NO₃⁻ concentration and low NH₄⁺ concentrations.
303 δ¹⁸O_{NO3-} of newly generated NO₃⁻ is tied to ambient water, making δ¹⁸O_{NO3-} a sensitive marker of
304 nitrification. We did not find evidence for parallel evolution of δ¹⁸O_{NO3-} and δ¹⁵N_{NO3-} along a 1:1 line
305 in groundwater samples, which was usually a strong signal of denitrification process. All the
306 sampled groundwater samples were oxic; however, their DO saturation ranged between 49% to
307 98%, indicating oxygenated groundwater condition was not homogenous across the downstream
308 area. Therefore, denitrification of groundwater NO₃⁻ in the coastal aquifer was plausible, as
309 theorized by Oehler, et al. ¹².

310 Groundwater PO₄³⁻ concentration in this study was similar compared to two years prior¹², which
311 was in a higher range than other sites in Indonesia⁶¹. High PO₄³⁻ concentration can be attributable
312 to fertilizer or wastewater input, both were presumably contributed to the elevated groundwater
313 NO₃⁻ concentration as well. In addition, natural sources also affect soluble PO₄³⁻ concentration in
314 groundwater. A recent study conducted in western Lombok found that in the absence of NH₄⁺
315 concentration in some parts of the island, the elevated groundwater PO₄³⁻ concentration was
316 derived from the dissolution of hydroxyapatite and/or vivianite minerals, which originated from
317 volcanic lava deposits of Mount Rinjani ⁶².

318 DSi concentrations in the coastal groundwater were in a range of 170-780 μM; however, two inland
319 spring samples from the mountain slope had DSi concentrations up to 1140 μM (Table 1, Figure
320 2). These inland springs receive their water from recharge at the slopes of Mt. Rinjani, and the

321 DSi enrichment in these samples is most likely due to water-rock interactions in the volcanic
322 aquifer⁶³. The different lithology between the mountain slope and coastal area can explain the one
323 magnitude DSi concentration difference between inland spring and coastal groundwater. For
324 instance, while the mountain slope aquifer is composed of quaternary volcanic rocks resulting in
325 elevated DSi concentration, the coastal aquifer is presumably characterized by a mix of volcanic
326 rocks and alluvial sand, which usually has a lower DSi range, e.g., 200 - 300 μM ⁶⁴. The varying
327 DSi concentration supports the previous notion that coastal groundwater was fed by several water
328 sources besides the inland springs we sampled.

329

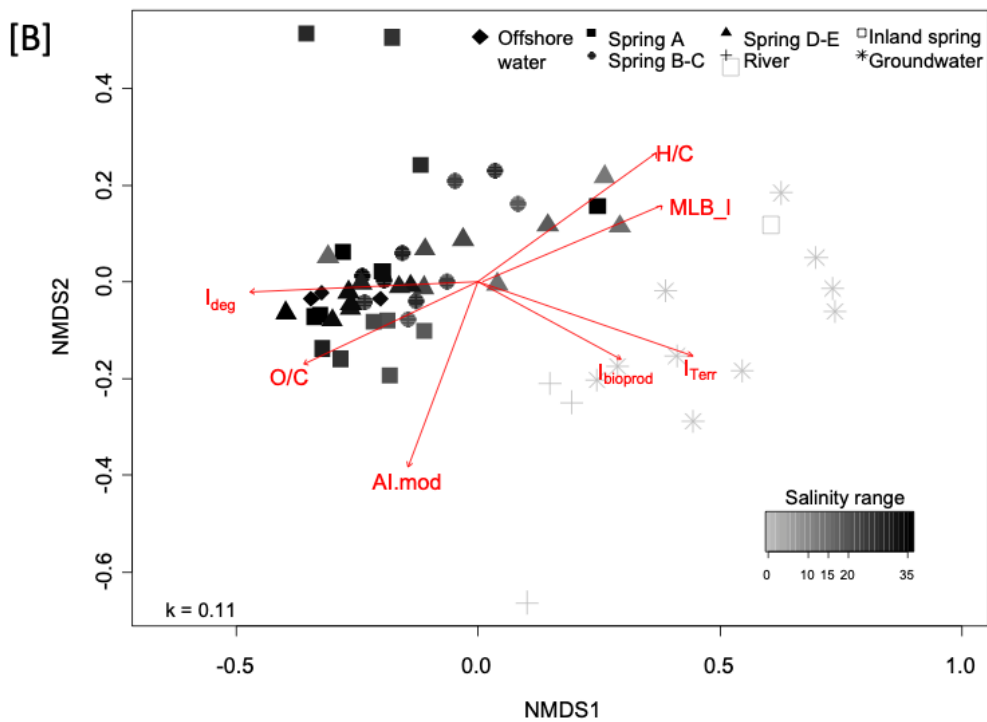
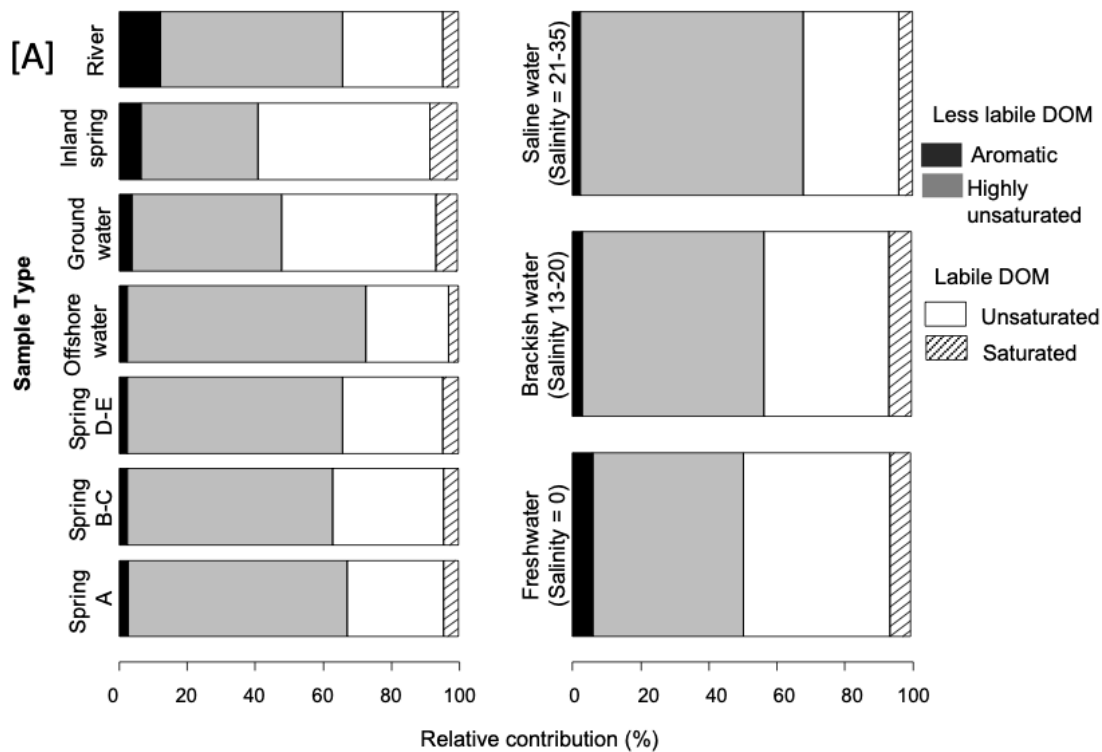
330 *DOC and DOM*

331 Coastal groundwater was characterized by DOC concentrations in the range of 65-200 μM , while
332 DON concentrations were between 0-60 μM . Figure 4A shows that the DOM pool in groundwater
333 was divided evenly between labile formulae (i.e., unsaturated aliphatic and saturated formulae)
334 and the less labile formulae (i.e., highly unsaturated and aromatic formulae⁵³). The unsaturated
335 aliphatics had the highest average relative composition of 48%, followed by highly unsaturated
336 (average relative contribution 41%), saturated (average relative contribution 6%), and aromatic
337 formulae (average relative contribution 4%). The prevalence of unsaturated aliphatics in
338 groundwater was consistent with previous studies conducted in fissured aquifers, where DOM
339 tends to be enriched with labile, unsaturated aliphatic compounds in this geological setting^{19,65}.
340 The low abundances of aromatic formulae in the volcanic aquifer can be caused by the soil
341 column's retention as aromatic-rich surface water percolates into the aquifer⁶⁶. DOM sorption to
342 soils, especially to iron hydroxides abundantly found in volcanic soil, can efficiently remove
343 aromatics and carboxyl moieties^{67,68}. In these cases, preferential sorption of the hydrophobic
344 fraction of aromatic DOM, which consists of high molecular weight, humic substances, and
345 vascular plant-derived matters, causes the aquifer to contain more aliphatic organic matter relative
346 to surface water⁶⁹.

347 Freshwater samples were characterized by high indices of I_{bioprod} , MLB.I, H/C ratios, and I_{Terr}
348 (Figure 4B, Supplementary Material). The occurrence of simultaneously high lability indices
349 (MLB.I, and H/C ratios) with high microbial production (I_{bioprod}) in groundwater samples indicates
350 that labile DOM was autochthonously produced in the aquifer^{19,65} or in the soils before entering
351 the aquifer by microbial activities⁷⁰. For example, soil fungi and bacteria are found to be capable
352 in altering and remineralizing DOM components during their percolation through the soil⁷¹.
353 Biologically reworked DOM in soils tend to be hydrogenated (high H/C ratios) and less likely to be
354 retained by soil minerals, resulting in elevated H/C ratio in groundwater DOM⁷⁰.

355 A surprisingly high I_{Terr} index was observed in the groundwater samples (range 0.54 - 0.76), even
356 comparable to river samples (ranged 0.63 - 0.69). A high groundwater I_{Terr} index is usually
357 associated with peat-influenced groundwater⁷², which was not the case in Lombok. As I_{Terr}
358 calculation was originated from Amazonian surface water samples⁵², it is usually correlated to high
359 aromaticity and may not be suitable to characterize groundwater attributes, as also observed in
360 another STE study⁷³. In contrast to groundwater samples, river samples contained elevated
361 aromatic compound abundances, up to twofold higher than any other type of sample (Figure 4A).
362 This finding is attributable to the fact that most aromatic pool is composed of vegetal or plant-
363 derived organic matter directly deposited in the rivers through leaf litter.

364



365

366 **Figure 4.** (A) Relative, intensity-weighted contributions of DOM molecular groups across end
 367 members and samples. (B) NMDS plot based on Bray-Curtis dissimilarity of the relative
 368 abundance of all DOM molecular formulae in each sample, color coded by respective sample
 369 salinities (bottom). Red arrows indicate the association of specific DOM molecular
 370 characteristics (indices, elemental ratios, aromaticity) with different sample groups.

371 An NMDS plot based on DOM molecular composition shows that the samples were grouped by
372 their salinity (Figure 4B). All the freshwater samples such as groundwater, river, and inland spring
373 samples were plotted on the right side of NMDS. Samples collected from discharge points were
374 plotted in the middle of the plot, while the high salinity samples were clustered on the opposite
375 side of freshwater samples. DistLM results applied to all samples indicated that differences in
376 salinity and temperature shaped the DOM molecular composition shift. In total, 25.59% of DOM
377 composition variability was explained by the observed parameters (Table 1). Salinity was the most
378 significant contributor shaping DOM molecular composition distribution between these parameters
379 with up to 13.49% contribution. Interestingly, a similar approach applied to only SGD samples
380 resulted in almost identical outcomes, where salinity and temperature were the determinant
381 contributors. DistLM applied to freshwater samples shows that pH was the primary variable
382 explaining DOM molecular composition with 23.49% total explainable variances. This finding is
383 consistent with other studies investigating pH as the main driver of the molecular differences
384 between DOM, particularly in terrestrial surface and pore water^{74,75}. We did not find significant
385 results when conducting this approach for groundwater samples only.

386 Overall, all of DistLM calculations resulted in a total explainable variance of below 30%, suggesting
387 that additional factors may control the DOM molecular distribution that we did not measure or
388 analyze (i.e., source heterogeneity). Such factors include soil type, microbial transformations, or
389 other abiotic processes such as flocculation, adsorption, desorption and photochemistry^{76,77}; the
390 latter particularly could be significant in seawater.

391 Table 1. Contribution and significance of observed environmental factors shaping DOM
392 composition based on DistLM

Source of variation	Adjusted R ² (%)	Df	F	p-value
All samples				
Final model	25.59	2	8.47	0.001 ***
Salinity	13.49	1	8.89	0.001 ***
Temperature	5.38	1	3.55	0.001 ***
SGD samples				
Final model	22.37	2	4.61	0.001 ***
Salinity	14.07	1	5.80	0.001 ***
Temperature	12.69	1	5.23	0.001 ***
Fresh water samples (groundwater, inland spring, river)				

Source of variation	Adjusted R ² (%)	Df	F	p-value
Final model	23.49	1	1.84	0.001 ***
pH	14.62	1	1.29	0.001 ***

393

394 **Biogeochemistry of submarine springs and reef water column**

395 *Submarine spring groundwater source*

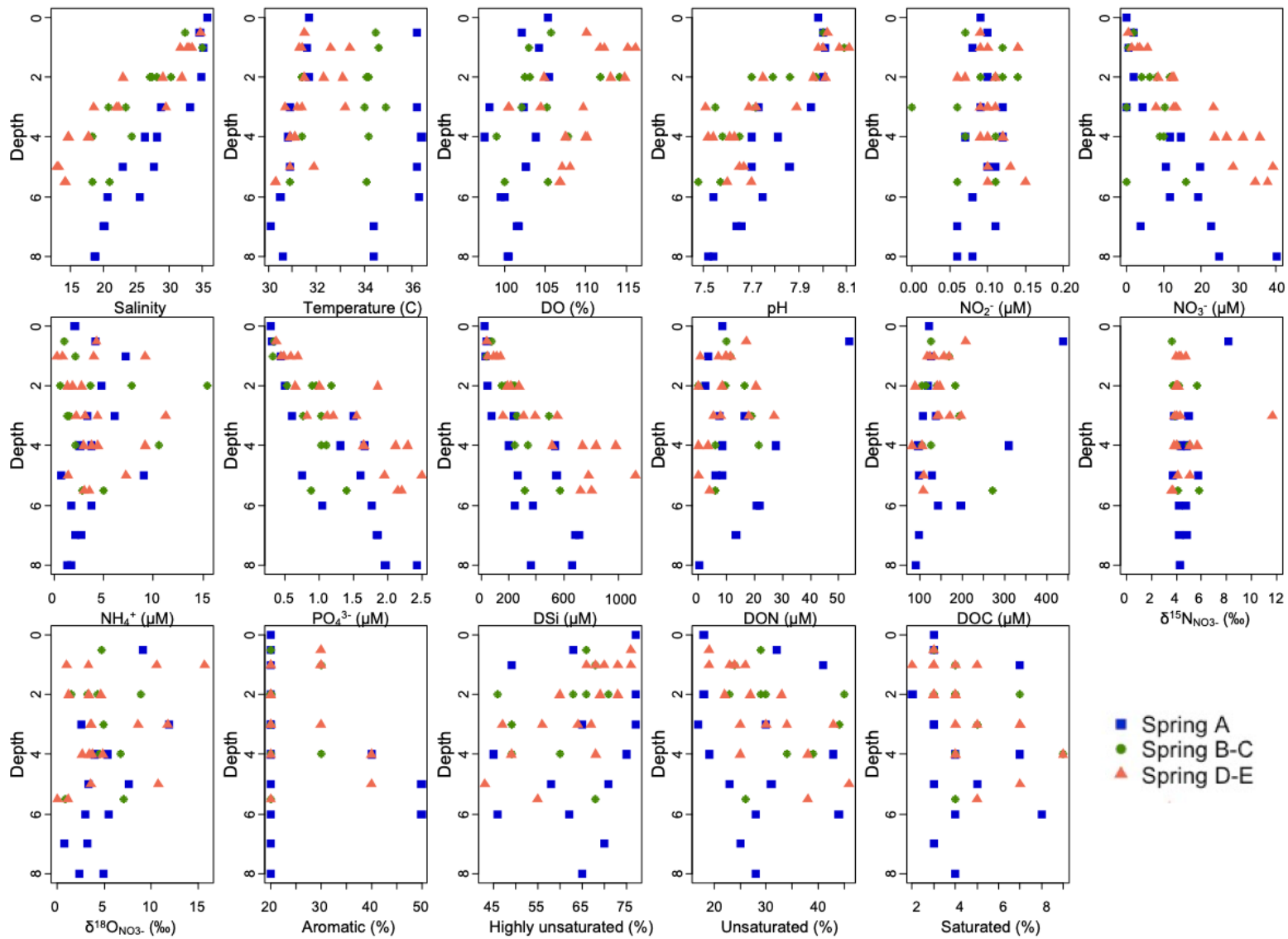
396 A previous study in northern Lombok found that nutrient concentrations behaved non-
 397 conservatively between fresh groundwater on land and discharging groundwater in the reef, i.e.,
 398 e.g., NO₃⁻ removal by denitrification or biological uptake¹². It was observed that the underlying
 399 mechanisms for these dynamics are either reactions in the coastal aquifer and the STE or different
 400 sources of water for the submarine springs. This study provides detailed insights into the
 401 previously hypothesized processes.

402 In general, submarine springs and reef water columns were characterized with warmer
 403 temperature than coastal groundwater (range 30 – 36 °C), medium pH (range 7.4 – 8.1), and
 404 oxygenated conditions (range 90-115%) (Figure 2). Salinity increased from brackish in the SGD
 405 discharge points (salinity = 13 - 20) to marine salinity at the surface water (salinity = 35) (Figure
 406 5). Salinity was more enriched in the submarine spring discharge points (salinity = 13 - 20) than
 407 in groundwater (salinity = 0) due to recirculated seawater in the STE. In every spring, salinity and
 408 pH increased from the discharge point towards the surface water (Figure 5). This pattern was
 409 followed by temperature and DO, albeit with a slighter increase. Our data revealed that
 410 groundwater discharging via submarine springs generally had a lower pH than the surrounding
 411 reef water. A pH as low as 7.7 is considered a threat to the coral reef system, as it is detrimental
 412 to calcifier recruitment and reef builders⁷⁸. Therefore, the relatively low pH delivered by SGD may
 413 promote coral acidification in the long term in this ecosystem.

414 The geochemistry of groundwater discharging via submarine springs differed between locations,
 415 particularly in salinity, DSi concentration, and DOM composition. Figure 5 shows that Springs D-
 416 E had slightly lower salinity at the discharge point (i.e., D1 and E1, salinity = 13-14) compared to
 417 Springs A, B, and C (salinity = 18-20) in both of sampling periods. The different pattern between

418 Springs A, B, C and Springs D-E discharge points was also displayed by DSi concentrations,
419 where its concentration ranged between 246 - 712 μM in Springs A, B, and C, while DSi
420 concentrations in Springs D-E amounted to 720 - 1121 μM or almost thrice the concentration in
421 Spring A. This concentration was higher than expected based on conservative mixing and even
422 comparable with the range of springs sampled in the hinterland at the lower slope of Mt. Rinjani.
423 Characteristics revealed by the DOM molecular properties also showed that the discharge points
424 of Springs D-E had a higher relative proportion of labile molecular formulae compared to Springs
425 A, B, and C (Figure 5). The possible explanations for this finding were (1) specific processes
426 occurred in the STE of Springs D-E adding significant amount of DSi, such as dissolution of
427 lithogenic particles or biogenic silica⁷⁹, and/or (2) Springs D-E were fed by different sources than
428 Springs A, B, C. This would support previous reports of different groundwater sources feeding the
429 spring complex by Oehler, et al. ¹². For instance, this study found that Spring A had a similar $\delta^{18}\text{O}$ -
430 H_2O and radon signature with coastal groundwater; thus, it potentially received groundwater from
431 the coastal catchment area. In contrast, Springs D-E may have received water from confined or
432 semi-confined aquifers in the hinterland as they consisted of heavier $\delta^{18}\text{O}$ - H_2O isotopic
433 composition and had higher radon activities. The different aquifers feeding coastal water are
434 reportedly typical for tropical volcanic islands⁸⁰.

435



436

437

Figure 5. Vertical depth profile of physicochemical parameters in submarine springs.

438 *Nutrients*

439 Nutrient samples were collected from the submarine spring plumes, i.e., from discharge point to
440 surface water, from two sampling periods. Statistical analyses showed no significant difference in
441 dissolved inorganic nutrient concentrations between two sampling periods (Wilcox test, $n = 66$, p
442 > 0.05). DON composed the major species of the dissolved nitrogen pool in the submarine springs
443 and reef water with a concentration between 0 - 54 μM , followed by NO_3^- (range 0-40 μM), NH_4^+
444 (range 0-15 μM), and NO_2^- (0-0.15 μM) (Figure 2).

445 In submarine springs and reef water columns, NO_3^- concentration was one magnitude lower than
446 in coastal groundwater. In general, NO_3^- concentration had a significant correlation with salinity
447 (Spearman $\rho = -0.87$, $n = 66$, p -value < 0.001), which indicates that NO_3^- in the submarine springs
448 originated from the groundwater. NO_3^- concentrations were elevated at the discharge point of
449 submarine springs; however, its relative composition in the bulk N decreased towards higher
450 salinity and reached 0 μM in the sampling points closest to the surface (Figure 5).

451 $\delta^{15}\text{N}_{\text{NO}_3^-}$ values were almost uniform on either end of the salinity scale (Figure 3B). The majority
452 of $\delta^{15}\text{N}_{\text{NO}_3^-}$ values in submarine springs and reef water column (+3‰ to +5‰) was similar with
453 $\delta^{15}\text{N}_{\text{NO}_3^-}$ in coastal groundwater, indicating similar, terrestrial NO_3^- origin. The $\delta^{18}\text{O}_{\text{NO}_3^-}$ values in
454 submarine springs and reef water (range -4‰ to +15‰) were generally distributed over a wider
455 range and were enriched in comparison to coastal groundwater (range -0‰ to +4‰).

456 Despite uncertainties regarding the inland source end-member assessment, we find that within
457 the submarine springs and reef water column, NO_3^- concentration plotted against theoretical
458 mixing line suggested non-conservative behavior. We rule out two NO_3^- sink pathways, i.e.,
459 denitrification or dissimilatory nitrate reduction to ammonia (DNRA), in the reef water column due
460 to the well-mixed, oxygenated condition in the water column. However, no data were available for
461 the intermediate salinity range from 1 to 15, which would occur in the STE. Therefore, we could
462 not exclude possible denitrification or DNRA in this salinity interval. For example, denitrification
463 could occur in the anoxic pockets of the STE sediments, and it would not result in any apparent

464 isotopic fractionation in the water samples because the diffusion of NO_3^- into reactive sediment
465 zones is the rate-limiting step⁸¹.

466 Figure 3B also shows that both $\delta^{15}\text{N}_{\text{NO}_3^-}$ and $\delta^{18}\text{O}_{\text{NO}_3^-}$ values deviated from the theoretical
467 conservative mixing line. $\delta^{15}\text{N}_{\text{NO}_3^-}$ values were slightly below the mixing line, while $\delta^{18}\text{O}_{\text{NO}_3^-}$ values
468 were generally enriched compared to conservative mixing. We did not observe any specific pattern
469 of depth or discharge from specific springs in the scatter plots. The low $\delta^{15}\text{N}_{\text{NO}_3^-}$ values in the
470 submarine springs and reef water, i.e., below the average marine $\delta^{15}\text{N}_{\text{NO}_3^-}$ of +5 ‰ in the region⁸²,
471 could be explained by: (1) a balance between consumption (assimilation, denitrification) that may
472 isotopically enrich NO_3^- and NO_3^- production (nitrification) that may reduce the isotopic value, or
473 (2) the prevalence of N_2 fixation.

474 The (albeit low) increase in NO_2^- concentration in Figure 5 suggests active NO_3^- turnover in the
475 reef water column. However, we did not find a clear trend in the enrichment of $\delta^{15}\text{N}_{\text{NO}_3^-}$ versus
476 $\delta^{18}\text{O}_{\text{NO}_3^-}$, which would be inarguable proof of active consumption. We found a slight relative
477 enrichment of $\delta^{18}\text{O}_{\text{NO}_3^-}$ versus $\delta^{15}\text{N}_{\text{NO}_3^-}$ along a slope of ~ 0.8: 1. Enrichment is close to the slope
478 of 1: 1 that is proposed for NO_3^- assimilation. We assume that assimilation occurs in the water
479 column but that the isotope signatures of N and O are partly decoupled due to the co-occurrence
480 of nitrification and assimilation in the water column⁸³. Additional isotopically light N might derive
481 from N_2 fixation, consistent with the elevated NH_4^+ concentration and the low DIN: PO_4^{3-} ratio in
482 reef surface water.

483 In contrast with NO_3^- , NO_2^- and NH_4^+ were generally enriched in the submarine springs and reef
484 water compared to groundwater (Figure 2). NO_2^- concentrations were below 0.05 μM in all
485 groundwater samples, while its concentration was between 0.05 - 0.5 μM in submarine springs
486 and reef water columns and appeared stable throughout the SGD vertical depth profile (Figure 5).
487 The relatively higher concentration of NO_2^- was presumably related to the active turnover of NO_3^-
488 in the water columns. Meanwhile, NH_4^+ concentrations ranged between 0-15 μM in the submarine
489 springs and reef water columns, compared to its concentration below LOD in all groundwater

490 samples. However, we observe slight enrichment of NH_4^+ vertical depth profile (Figure 5), which
491 can be attributable to the production of NH_4^+ from the mineralization of marine organic matter⁸⁴.
492 NH_4^+ is also commonly found as a DOM photoproduct^{85,86}, which may define their slight
493 enrichment in the upper level of the seawater column and offshore water (Figure 2). The
494 enrichment of NH_4^+ in the reef water column is rather surprising, considering NH_4^+ is usually
495 preferred by phytoplankton or other heterotrophic microorganisms over NO_3^- . We assume that the
496 uptake and recycling of NH_4^+ in the upper water column are partially inhibited by light limitation of
497 nitrifiers or varying DIN preferences depending on the biota species⁸⁷.
498 Like NO_3^- , PO_4^{3-} concentrations in submarine springs and reef water were one magnitude lower
499 than in coastal groundwater (Figure 2). Overall, PO_4^{3-} concentration was negatively correlated with
500 salinity (Spearman $\rho = -0.88$, $n = 66$, $p < 0.001$) and PO_4^{3-} concentration plotted against salinity
501 suggested non-conservative behavior. During its transport from land to ocean, PO_4^{3-} could be
502 attenuated in the STE as it has high affinity with iron oxide⁸⁸, which was potentially abundant in a
503 volcanic island. In the reef water, SGD vertical depth profile shows higher PO_4^{3-} concentration in
504 deeper depth/SGD discharge points compared to surface water (Figure 5). Coupled with non-
505 conservative mixing behavior, this finding indicates possible PO_4^{3-} biological uptake in the water
506 column. At the time of our sampling expedition, DIN: PO_4^{3-} ratios of brackish and saline samples
507 were in the range of 1 – 28, with P-limitation occurring in samples taken close to submarine springs
508 and N-limitation dominating in the surface seawater column.
509 Overall, findings from nutrient data suggest that in a well-mixed, sunlit coastal water, groundwater-
510 derived nutrients may experience rapid turnover from the discharge point to the surface water
511 column.

512
513 *DOC and DOM*
514 In submarine springs and reef water column, DOC and DON were measured in the range of 82 –
515 437 μM and 0 - 54 μM , respectively. Overall, the molecular composition of DOM in submarine

516 springs and reef water was distinctly different from that in the groundwater samples (Figure 4A).
517 For example, the relative contribution of all formulae shifted from groundwater samples to SGD
518 discharge points: aromatics (4% to 2%), highly unsaturated (44% to 58%), unsaturated (45% to
519 34%), and saturated (6% to 4%). In general, the biggest relative contribution shifts were
520 experienced by highly unsaturated (14% increase) and unsaturated compounds (11% decrease)
521 during their transport in the STE. In the same interval, we also observed a decrease of DON (130
522 to 110 μM) and an increase of I_{deg} from lower to higher degradation state (0.2 to 0.4). This finding
523 suggests that the DOC supplied by the groundwater, mostly the labile ones, was actively utilized
524 or degraded in the STE. Furthermore, the slight removal of aromatic compounds could be
525 attributable to adsorption to iron oxide in the STE⁸⁹.

526 In the submarine springs and reef water, DOC concentration was also mostly homogenous along
527 the SGD vertical depth profile, except for mid- and upper- depth samples from Spring A (Figure
528 5). Therefore, tight coupling is assumed between DOC consumption and production in the reef
529 water. The less labile fraction dominated DOM composition in the reef water column: the highly
530 unsaturated formulae were prevalent in all submarine springs and reef water column with an
531 average relative contribution of 63% (Figure 4A), and their proportion increased from deeper
532 towards the upper layer of reef water, particularly in Springs D-E (Figure 5). Unsaturated aliphatics
533 composed the second-highest composition of these samples (average relative contribution of
534 30%), followed by saturated (average relative contribution 4%) and aromatic (average relative
535 contribution of 3%) formulae (Figure 4A). The unsaturated aliphatic relative composed 30%
536 relative contribution of reef water samples indicates that labile DOC was produced in the reef
537 water, e.g., from phytoplankton or reef organisms⁹⁰. As aromatic compounds in this study were
538 highly enriched in river water, their low abundance in reef water indicates no surface runoff
539 contribution to the coral reef ecosystem at the time of our study.

540 Submarine springs and reef water DOM samples were distinguished by relatively high O/C ratios
541 and an elevated degradation index (I_{deg}) (Figure 4B). A simultaneous increase of I_{deg} and highly

542 unsaturated formulae in the vertical depth profile indicates increasing amounts of reworked DOM
543 from the bottom to the top layer of the water column. The enrichment of less labile formulae could
544 originate from rapid microbial degradation of labile compounds⁹¹, reef production⁹⁰ or physical
545 processes such as remineralization or photochemical activity. We also cannot rule out the
546 influence of horizontal water exchange with the open sea, as the oceanic endmember had the
547 highest relative contribution of highly unsaturated formulae (Figure 4A). The highly unsaturated
548 formulae could consist of carboxyl-rich alicyclic molecules (CRAM), a type of degraded DOM often
549 found in the open sea that derives from non-aromatic OM decomposition^{92,93} or photochemical
550 products in seawater^{94,95}. CRAM in the coral reef ecosystem can be resistant to degradation on
551 the scale of weeks⁹⁶ to months⁹⁰.

552

553 **Implications for the coral reef ecosystem**

554 Considering the socio-anthropogenic development in northern Lombok, it is surprising how
555 consistent some of the nutrient concentrations behave with time. While nutrient concentrations in
556 karstic coastal aquifers usually vary over time scales of days to weeks⁹⁷, the result from Spring A
557 showed similar salinity, DSi, and NO_3^- concentrations when compared with the study by Oehler,
558 et al. ¹², where samples were taken four years ago during a different season. Therefore, we
559 assume that the submarine springs provide a constant delivery of DSi, NO_3^- , and PO_4^{3-} into the
560 coral reef regardless of the season.

561 In this study, we observe anthropogenic influence on the groundwater system in Lombok. An
562 annual population growth of 1.1% per year and an urbanization rate of 5.5% per year is predicted
563 for Lombok, which is even faster than the Indonesian megacity of Jakarta⁹⁸. Therefore, it is likely
564 that inputs of anthropogenic pollutants to groundwater, and hence via SGD to coastal water, will
565 increase. At the study site, the early symptoms of coral health disturbance have already been
566 discovered: a local study found an elevated algal cover on the coral reef in Spring A³⁷. In this
567 location, algae cover 30.85% of the total coral ecosystem, compared to 19.21% coverage in

568 Springs B-C. In many cases, the algal cover was attributable to excess nutrients and DOC,
569 particularly labile DOC, as they stimulate the growth of non-calcifying turf algae and fleshy
570 macroalgae⁹⁹. In the long term, an increase of algal cover instead of calcifying organisms may
571 cause the prevalence of copiotrophic organisms and often potentially virulent microbial
572 populations¹⁰⁰. Therefore, future environmental management should include measuring nutrient
573 and organic matter concentration to prevent coral mortality cases.

574

575 **CONCLUSIONS**

576 Overall, our study points to the role of SGD in delivering nutrients and labile DOM into the coral
577 reef ecosystem. We observed that the composition of nutrient and DOM pool transported by SGD
578 changed in the submarine springs and reef water due to biology (fixation, production, and uptake),
579 hydrology (dilution, mixing), and diagenetic processing (degradation). This study may lay a
580 foundation for more in-depth research on groundwater sources and pathways, SGD-derived
581 nutrients and DOM bioavailability and uptake potential in the coral reef, and subsequently the
582 association between SGD and coral health. In particular, other countries in the Coral Triangle
583 marine area are categorized as either low or middle economy countries, usually associated with
584 densely populated coastal areas with limited environmental measures for land-based pollution.
585 However, as far as we know, only two studies associating SGD-derived anthropogenic nutrients
586 with the coral reef ecosystem in this region, i.e., in Indonesia¹² and the Philippines¹⁰¹. Going
587 forward, considering coral reef ecosystems is highly sensitive to terrestrial anthropogenic activities
588 and global climate change, strong attention has to be paid to addressing these knowledge gaps
589 not only in the Coral Triangle region but also in similar tropical ecosystems worldwide.

590

591 **Acknowledgment**

592 We are grateful for the assistance in the field by Dr. Eko Pradjoko and Dr. I Wayan Yasa from
593 University of Mataram, as well as student assistants Anisa Nindyasari, Fawqa Anugerah, Alan

594 Maulana, and Jarrid Tschaikowski for their help in sample collection. We thank Matthias Birkicht
595 (ZMT), Markus Ankele (HZG), Ina Ulber (ICBM), Matthias Friebe (ICBM), and Katrin Klapproth
596 (ICBM) for their assistance with nutrient, NO₃⁻ isotope, DOC, and DOM analyses. DA is funded by
597 the German Research Foundation through Walter Benjamin Fellowship (#446330207). HW is
598 funded by the Niedersächsisches Ministerium für Wissenschaft und Kultur (MWK) in the scope of
599 project "BIME" (ZN3184). This project was funded by German Federal Ministry for Education and
600 Science (BMBF Grant No #01LN1307A to Nils Moosdorf).

601 Supporting Information

602 The supporting information (Supplementary Table on Data Measurement and DOM Molecular
603 Composition for each of the samples) is available free of charge via the internet at
604 <https://pubs.acs.org/>.

605 References

- 606 1 Church, T. M. An underground route for the water cycle. *Nature* **380**, 579-580 (1996).
- 607 2 Moore, W. S. The effect of submarine groundwater discharge on the ocean. *Annual review of*
608 *marine science* **2**, 59-88 (2010).
- 609 3 Kwon, E. Y. *et al.* Global estimate of submarine groundwater discharge based on an
610 observationally constrained radium isotope model. *Geophysical Research Letters* **41**, 8438-8444
611 (2014).
- 612 4 Luijendijk, E., Gleeson, T. & Moosdorf, N. Fresh groundwater discharge insignificant for the
613 world's oceans but important for coastal ecosystems. *Nature communications* **11**, 1-12 (2020).
- 614 5 Slomp, C. P. & Van Cappellen, P. Nutrient inputs to the coastal ocean through submarine
615 groundwater discharge: controls and potential impact. *Journal of Hydrology* **295**, 64-86 (2004).
- 616 6 Windom, H. L., Moore, W. S., Niencheski, L. F. H. & Jahnke, R. A. Submarine groundwater
617 discharge: A large, previously unrecognized source of dissolved iron to the South Atlantic Ocean.
618 *Marine Chemistry* **102**, 252-266 (2006).
- 619 7 Kim, J. & Kim, G. Inputs of humic fluorescent dissolved organic matter via submarine
620 groundwater discharge to coastal waters off a volcanic island (Jeju, Korea). *Scientific reports* **7**, 1-
621 9 (2017).
- 622 8 Boehm, A. B., Shellenbarger, G. G. & Paytan, A. Groundwater discharge: potential association
623 with fecal indicator bacteria in the surf zone. *Environmental science & technology* **38**, 3558-3566
624 (2004).
- 625 9 Paerl, H. W. Coastal eutrophication and harmful algal blooms: Importance of atmospheric
626 deposition and groundwater as "new" nitrogen and other nutrient sources. *Limnology and*
627 *oceanography* **42**, 1154-1165 (1997).

- 628 10 Lecher, A. L. & Mackey, K. R. Synthesizing the effects of submarine groundwater discharge on
629 marine biota. *Hydrology* **5**, 60 (2018).
- 630 11 Carruthers, T. J. B., van Tussenbroek, B. I. & Dennison, W. C. Influence of submarine springs and
631 wastewater on nutrient dynamics of Caribbean seagrass meadows. *Estuarine, Coastal and Shelf*
632 *Science* **64**, 191-199, doi:<https://doi.org/10.1016/j.ecss.2005.01.015> (2005).
- 633 12 Oehler, T. *et al.* Nutrient dynamics in submarine groundwater discharge through a coral reef
634 (western Lombok, Indonesia). *Limnology and Oceanography* **64**, 2646-2661 (2019).
- 635 13 Moosdorf, N., Stieglitz, T., Waska, H., Dürr, H. H. & Hartmann, J. Submarine groundwater
636 discharge from tropical islands: a review. *Grundwasser* **20**, 53-67 (2015).
- 637 14 Elvidge, C. D. *et al.* Radiance calibration of DMSP-OLS low-light imaging data of human
638 settlements. *Remote Sensing of Environment* **68**, 77-88 (1999).
- 639 15 Fabricius, K. E. Effects of terrestrial runoff on the ecology of corals and coral reefs: review and
640 synthesis. *Marine Pollution Bulletin* **50**, 125-146,
641 doi:<https://doi.org/10.1016/j.marpolbul.2004.11.028> (2005).
- 642 16 D'Angelo, C. & Wiedenmann, J. Impacts of nutrient enrichment on coral reefs: new perspectives
643 and implications for coastal management and reef survival. *Current Opinion in Environmental*
644 *Sustainability* **7**, 82-93, doi:<https://doi.org/10.1016/j.cosust.2013.11.029> (2014).
- 645 17 Kline, D. I., Kuntz, N. M., Breitbart, M., Knowlton, N. & Rohwer, F. Role of elevated organic
646 carbon levels and microbial activity in coral mortality. *Marine Ecology Progress Series* **314**, 119-
647 125 (2006).
- 648 18 Kuntz, N. M., Kline, D. I., Sandin, S. A. & Rohwer, F. Pathologies and mortality rates caused by
649 organic carbon and nutrient stressors in three Caribbean coral species. *Marine Ecology Progress*
650 *Series* **294**, 173-180 (2005).
- 651 19 Tedetti, M., Cuet, P., Guigue, C. & Goutx, M. Characterization of dissolved organic matter in a
652 coral reef ecosystem subjected to anthropogenic pressures (La Réunion Island, Indian Ocean)
653 using multi-dimensional fluorescence spectroscopy. *Science of the total environment* **409**, 2198-
654 2210 (2011).
- 655 20 Nelson, C. E. *et al.* Fluorescent dissolved organic matter as a multivariate biogeochemical tracer
656 of submarine groundwater discharge in coral reef ecosystems. *Marine Chemistry* **177**, 232-243
657 (2015).
- 658 21 Hedges, J. I. *et al.* The molecularly-uncharacterized component of nonliving organic matter in
659 natural environments. *Organic geochemistry* **31**, 945-958 (2000).
- 660 22 Koch, B. P., Witt, M., Engbrodt, R., Dittmar, T. & Kattner, G. Molecular formulae of marine and
661 terrigenous dissolved organic matter detected by electrospray ionization Fourier transform ion
662 cyclotron resonance mass spectrometry. *Geochimica et Cosmochimica Acta* **69**, 3299-3308
663 (2005).
- 664 23 Longnecker, K. & Kujawinski, E. B. Composition of dissolved organic matter in groundwater.
665 *Geochimica et Cosmochimica Acta* **75**, 2752-2761 (2011).
- 666 24 Osterholz, H., Kirchman, D. L., Niggemann, J. & Dittmar, T. Environmental drivers of dissolved
667 organic matter molecular composition in the Delaware Estuary. *Frontiers in Earth Science* **4**, 95
668 (2016).
- 669 25 Lusk, M. G. & Toor, G. S. Dissolved organic nitrogen in urban streams: biodegradability and
670 molecular composition studies. *Water research* **96**, 225-235 (2016).
- 671 26 Seidel, M. *et al.* Benthic-pelagic coupling of nutrients and dissolved organic matter composition
672 in an intertidal sandy beach. *Marine Chemistry* **176**, 150-163 (2015).
- 673 27 Schmidt, F., Elvert, M., Koch, B. P., Witt, M. & Hinrichs, K.-U. Molecular characterization of
674 dissolved organic matter in pore water of continental shelf sediments. *Geochimica et*
675 *Cosmochimica Acta* **73**, 3337-3358 (2009).

- 676 28 Lechtenfeld, O. J. *et al.* Molecular transformation and degradation of refractory dissolved organic
677 matter in the Atlantic and Southern Ocean. *Geochimica et Cosmochimica Acta* **126**, 321-337
678 (2014).
- 679 29 Rossel, P. E., Bienhold, C., Boetius, A. & Dittmar, T. Dissolved organic matter in pore water of
680 Arctic Ocean sediments: Environmental influence on molecular composition. *Organic*
681 *Geochemistry* **97**, 41-52 (2016).
- 682 30 Seitzinger, S. P. *et al.* Global patterns of dissolved inorganic and particulate nitrogen inputs to
683 coastal systems: Recent conditions and future projections. *Estuaries* **25**, 640-655,
684 doi:10.1007/BF02804897 (2002).
- 685 31 Adyasari, D. *et al.* Anthropogenic impact on Indonesian coastal water and ecosystems: Current
686 status and future opportunities. *Marine Pollution Bulletin* **171**, 112689,
687 doi:<https://doi.org/10.1016/j.marpolbul.2021.112689> (2021).
- 688 32 Asian Development Bank. State of the Coral Triangle: Indonesia 84 (Asian Development Bank
689 Manila, Philippines, 2014).
- 690 33 Nugraha, G. U., Bakti, H., Lubis, R. F., Sudrajat, Y. & Arisbaya, I. Aquifer vulnerability in the
691 Coastal Northern Part of Lombok Island Indonesia. *Environment, Development and Sustainability*,
692 doi:10.1007/s10668-021-01459-0 (2021).
- 693 34 Matrais, I. B., Pfeiffer, D., Soekardi, R. & Stach, L. *Hydrogeology of the island of Lombok*
694 *(Indonesia)*. (Schweizerbart, 1972).
- 695 35 Lestiana, H., Sukristiyanti, S., Bakti, H. & Lubis, R. F. PEMANFAATAN BAND TERMAL CITRA
696 LANDSAT UNTUK IDENTIFIKASI KELUARAN AIR TANAH LEPAS PANTAI (KALP) DI PANTAI UTARA
697 LOMBOK. *2017* **27**, 11, doi:10.14203/risetgeotam2017.v27.422 (2017).
- 698 36 Lubis, R. F., Bakti, H. & Suriadarma, A. Submarine groundwater discharge in Indonesia. *Jurnal*
699 *RISSET Geologi dan Pertambangan* **21**, 57-62 (2011).
- 700 37 Johan, O., Kusumah, G. & Wisha, U. J. Kondisi Terumbu Karang di kawasan KALP Pantai Krakas,
701 Lombok Utara. *Jurnal Segara* **13**, doi:<http://dx.doi.org/10.15578/segara.v13i3.6548> (2017).
- 702 38 Moosdorf, N. & Oehler, T. Societal use of fresh submarine groundwater discharge: An
703 overlooked water resource. *Earth-Science Reviews* **171**, 338-348 (2017).
- 704 39 Grasshoff, K., Kremling, K. & Ehrhardt, M. *Methods of seawater analysis*. (John Wiley & Sons,
705 2009).
- 706 40 Sigman, D. M. *et al.* A bacterial method for the nitrogen isotopic analysis of nitrate in seawater
707 and freshwater. *Analytical chemistry* **73**, 4145-4153 (2001).
- 708 41 Casciotti, K. L., Sigman, D. M., Hastings, M. G., Böhlke, J. & Hilkert, A. Measurement of the
709 oxygen isotopic composition of nitrate in seawater and freshwater using the denitrifier method.
710 *Analytical Chemistry* **74**, 4905-4912 (2002).
- 711 42 Granger, J. & Sigman, D. M. Removal of nitrite with sulfamic acid for nitrate N and O isotope
712 analysis with the denitrifier method. *Rapid Communications in Mass Spectrometry: An*
713 *International Journal Devoted to the Rapid Dissemination of Up-to-the-Minute Research in Mass*
714 *Spectrometry* **23**, 3753-3762 (2009).
- 715 43 Böhlke, J., Mroczkowski, S. & Coplen, T. Oxygen isotopes in nitrate: New reference materials for
716 18O: 17O: 16O measurements and observations on nitrate-water equilibration. *Rapid*
717 *Communications in Mass Spectrometry* **17**, 1835-1846 (2003).
- 718 44 Sigman, D. M. *et al.* The dual isotopes of deep nitrate as a constraint on the cycle and budget of
719 oceanic fixed nitrogen. *Deep Sea Research Part I: Oceanographic Research Papers* **56**, 1419-1439
720 (2009).
- 721 45 Fry, B. Conservative mixing of stable isotopes across estuarine salinity gradients: a conceptual
722 framework for monitoring watershed influences on downstream fisheries production. *Estuaries*
723 **25**, 264-271 (2002).

724 46 Vandenberg, J., De Neve, S., Qualls, R. G., Salomez, J. & Hofman, G. Optimization of dissolved
725 organic nitrogen (DON) measurements in aqueous samples with high inorganic nitrogen
726 concentrations. *Science of the Total Environment* **386**, 103-113 (2007).

727 47 Dittmar, T., Koch, B., Hertkorn, N. & Kattner, G. A simple and efficient method for the solid-phase
728 extraction of dissolved organic matter (SPE-DOM) from seawater. *Limnology and Oceanography: Methods*
729 **6**, 230-235 (2008).

730 48 Merder, J. *et al.* ICBM-OCEAN: Processing Ultrahigh-Resolution Mass Spectrometry Data of
731 Complex Molecular Mixtures. *Analytical Chemistry* **92**, 6832-6838,
732 doi:10.1021/acs.analchem.9b05659 (2020).

733 49 Koch, B. & Dittmar, T. From mass to structure: An aromaticity index for high-resolution mass
734 data of natural organic matter. *Rapid communications in mass spectrometry* **20**, 926-932 (2006).

735 50 Rossel, P. E., Bienhold, C., Hehemann, L., Dittmar, T. & Boetius, A. Molecular Composition of
736 Dissolved Organic Matter in Sediment Porewater of the Arctic Deep-Sea Observatory
737 HAUSGARTEN (Fram Strait). *Frontiers in Marine Science* **7**, doi:10.3389/fmars.2020.00428 (2020).

738 51 Flerus, R. *et al.* A molecular perspective on the ageing of marine dissolved organic matter.
739 *Biogeosciences* **9**, 1935-1955 (2012).

740 52 Medeiros, P. M. *et al.* A novel molecular approach for tracing terrigenous dissolved organic
741 matter into the deep ocean. *Global Biogeochemical Cycles* **30**, 689-699,
742 doi:10.1002/2015GB005320 (2016).

743 53 D'Andrilli, J., Cooper, W. T., Foreman, C. M. & Marshall, A. G. An ultrahigh-resolution mass
744 spectrometry index to estimate natural organic matter lability. *Rapid Communications in Mass*
745 *Spectrometry* **29**, 2385-2401 (2015).

746 54 R Core Team. (R Foundation for Statistical Computing, Vienna, Austria, 2018).

747 55 Oksanen, J. *et al.* vegan: Community Ecology Package. R package version 2.5–6. (2019).

748 56 Kendall, C., Elliott, E. M. & Wankel, S. D. in *Stable Isotopes in Ecology and Environmental Science*
749 375-449 (2007).

750 57 Alshameri, A. *et al.* Adsorption of ammonium by different natural clay minerals: Characterization,
751 kinetics and adsorption isotherms. *Applied Clay Science* **159**, 83-93,
752 doi:<https://doi.org/10.1016/j.clay.2017.11.007> (2018).

753 58 NTB Bureau of Statistics. NTB dalam Angka ("NTB Province in Figures"). 434 (NTB Bureau of
754 Statistics, Mataram, 2020).

755 59 Katam. *Agricultural Cultivation Calendar*, <<http://katam.litbang.pertanian.go.id/>> (2020).

756 60 Ministry of Environment and Forestry. in *82/2001* (ed Ministry of Environment and Forestry)
757 (Jakarta, 2001).

758 61 Adyasari, D., Oehler, T., Afiati, N. & Moosdorf, N. Environmental impact of nutrient fluxes
759 associated with submarine groundwater discharge at an urbanized tropical coast. *Estuarine,
760 Coastal and Shelf Science* **221**, 30-38 (2019).

761 62 Ioka, S. *et al.* Species and potential sources of phosphorus in groundwater in and around
762 Mataram City, Lombok Island, Indonesia. *SN Applied Sciences* **3**, 27, doi:10.1007/s42452-020-
763 03975-6 (2021).

764 63 Schopka, H. H. & Derry, L. A. Chemical weathering fluxes from volcanic islands and the
765 importance of groundwater: The Hawaiian example. *Earth and Planetary Science Letters* **339**, 67-
766 78 (2012).

767 64 Rahman, S., Tamborski, J. J., Charette, M. A. & Cochran, J. K. Dissolved silica in the subterranean
768 estuary and the impact of submarine groundwater discharge on the global marine silica budget.
769 *Marine Chemistry* **208**, 29-42, doi:<https://doi.org/10.1016/j.marchem.2018.11.006> (2019).

770 65 Birdwell, J. E. & Engel, A. S. Characterization of dissolved organic matter in cave and spring
771 waters using UV-Vis absorbance and fluorescence spectroscopy. *Organic Geochemistry* **41**, 270-
772 280 (2010).

773 66 Osburn, C. L. *et al.* Regional groundwater and storms are hydrologic controls on the quality and
774 export of dissolved organic matter in two tropical rainforest streams, Costa Rica. *Journal of*
775 *Geophysical Research: Biogeosciences* **123**, 850-866 (2018).

776 67 Kaiser, K., Guggenberger, G., Haumaier, L. & Zech, W. Dissolved organic matter sorption on sub
777 soils and minerals studied by ¹³C-NMR and DRIFT spectroscopy. *European Journal of Soil Science*
778 **48**, 301-310 (1997).

779 68 Kaiser, K., Guggenberger, G. & Zech, W. Sorption of DOM and DOM fractions to forest soils.
780 *Geoderma* **74**, 281-303 (1996).

781 69 Cory, R., Green, S. & Pregitzer, K. Dissolved organic matter concentration and composition in the
782 forests and streams of Olympic National Park, WA. *Biogeochemistry* **67**, 269-288 (2004).

783 70 Shen, Y., Chapelle, F. H., Strom, E. W. & Benner, R. Origins and bioavailability of dissolved organic
784 matter in groundwater. *Biogeochemistry* **122**, 61-78, doi:10.1007/s10533-014-0029-4 (2015).

785 71 Kalbitz, K., Solinger, S., Park, J.-H., Michalzik, B. & Matzner, E. Controls on the dynamics of
786 dissolved organic matter in soils: a review. *Soil science* **165**, 277-304 (2000).

787 72 Riedel, T., Biester, H. & Dittmar, T. Molecular fractionation of dissolved organic matter with
788 metal salts. *Environmental Science & Technology* **46**, 4419-4426 (2012).

789 73 Waska, H. *et al.* Molecular Traits of Dissolved Organic Matter in the Subterranean Estuary of a
790 High-Energy Beach: Indications of Sources and Sinks. *Frontiers in Marine Science* **8**,
791 doi:10.3389/fmars.2021.607083 (2021).

792 74 Roth, V.-N., Dittmar, T., Gaupp, R. & Gleixner, G. Latitude and pH driven trends in the molecular
793 composition of DOM across a north south transect along the Yenisei River. *Geochimica et*
794 *Cosmochimica Acta* **123**, 93-105 (2013).

795 75 Roth, V.-N., Dittmar, T., Gaupp, R. & Gleixner, G. The molecular composition of dissolved organic
796 matter in forest soils as a function of pH and temperature. *PLoS One* **10**, e0119188 (2015).

797 76 Hernes, P. J. & Benner, R. Photochemical and microbial degradation of dissolved lignin phenols:
798 Implications for the fate of terrigenous dissolved organic matter in marine environments. *Journal*
799 *of Geophysical Research: Oceans* **108**, doi:10.1029/2002JC001421 (2003).

800 77 Keil, R. G., Montluçon, D. B., Prah, F. G. & Hedges, J. I. Sorptive preservation of labile organic
801 matter in marine sediments. *Nature* **370**, 549-552 (1994).

802 78 Kleypas, J. A. & Langdon, C. Coral reefs and changing seawater carbonate chemistry. *Coastal and*
803 *Estuarine Studies: Coral Reefs and Climate Change Science and Management* **61**, 73-110 (2006).

804 79 Ehlert, C. *et al.* Transformation of silicon in a sandy beach ecosystem: Insights from stable silicon
805 isotopes from fresh and saline groundwaters. *Chemical Geology* **440**, 207-218 (2016).

806 80 Hagedorn, B., Becker, M. W. & Silbiger, N. J. Evidence of freshened groundwater below a tropical
807 fringing reef. *Hydrogeology Journal*, 1-17 (2020).

808 81 Brandes, J. A. & Devol, A. H. Isotopic fractionation of oxygen and nitrogen in coastal marine
809 sediments. *Geochimica et Cosmochimica Acta* **61**, 1793-1801 (1997).

810 82 Sigman, D. M., Altabet, M., McCorkle, D., Francois, R. & Fischer, G. The $\delta^{15}\text{N}$ of nitrate in the
811 Southern Ocean: Nitrogen cycling and circulation in the ocean interior. *Journal of Geophysical*
812 *Research: Oceans* **105**, 19599-19614 (2000).

813 83 Wankel, S. D., Kendall, C., Pennington, J. T., Chavez, F. P. & Paytan, A. Nitrification in the
814 euphotic zone as evidenced by nitrate dual isotopic composition: Observations from Monterey
815 Bay, California. *Global Biogeochemical Cycles* **21**, doi:<https://doi.org/10.1029/2006GB002723>
816 (2007).

817 84 Froelich, P. N. *et al.* Early oxidation of organic matter in pelagic sediments of the eastern
818 equatorial Atlantic: suboxic diagenesis. *Geochimica et cosmochimica acta* **43**, 1075-1090 (1979).

819 85 Bushaw, K. L. *et al.* Photochemical release of biologically available nitrogen from aquatic
820 dissolved organic matter. *Nature* **381**, 404-407 (1996).

821 86 Moran, M. A. & Zepp, R. G. Role of photoreactions in the formation of biologically labile
822 compounds from dissolved organic matter. *Limnology and Oceanography* **42**, 1307-1316 (1997).
823 87 Dortch, Q. The interaction between ammonium and nitrate uptake in phytoplankton. *Marine*
824 *Ecology Progress Series* **61**, 183-201 (1990).
825 88 Domagalski, J. L. & Johnson, H. M. Subsurface transport of orthophosphate in five agricultural
826 watersheds, USA. *Journal of Hydrology* **409**, 157-171 (2011).
827 89 Linkhorst, A., Dittmar, T. & Waska, H. Molecular fractionation of dissolved organic matter in a
828 shallow subterranean estuary: the role of the iron curtain. *Environmental Science & Technology*
829 **51**, 1312-1320 (2017).
830 90 Tanaka, Y., Ogawa, H. & Miyajima, T. Production and bacterial decomposition of dissolved
831 organic matter in a fringing coral reef. *Journal of oceanography* **67**, 427-437 (2011).
832 91 Hansell, D. A., Kadko, D. & Bates, N. R. Degradation of Terrigenous Dissolved Organic Carbon in
833 the Western Arctic Ocean. *Science* **304**, 858, doi:10.1126/science.1096175 (2004).
834 92 Kang, P.-G. & Mitchell, M. J. Bioavailability and size-fraction of dissolved organic carbon,
835 nitrogen, and sulfur at the Arbutus Lake watershed, Adirondack Mountains, NY. *Biogeochemistry*
836 **115**, 213-234 (2013).
837 93 Fellman, J. B., D'Amore, D. V., Hood, E. & Boone, R. D. Fluorescence characteristics and
838 biodegradability of dissolved organic matter in forest and wetland soils from coastal temperate
839 watersheds in southeast Alaska. *Biogeochemistry* **88**, 169-184 (2008).
840 94 Hertkorn, N. *et al.* Characterization of a major refractory component of marine dissolved organic
841 matter. *Geochimica et Cosmochimica Acta* **70**, 2990-3010 (2006).
842 95 Kieber, R. J., Hydro, L. H. & Seaton, P. J. Photooxidation of triglycerides and fatty acids in
843 seawater: Implication toward the formation of marine humic substances. *Limnology and*
844 *Oceanography* **42**, 1454-1462 (1997).
845 96 Vacelet, E. & Thomassin, B. A. Microbial utilization of coral mucus in long term in situ incubation
846 over a coral reef. *Hydrobiologia* **211**, 19-32 (1991).
847 97 Oehler, T. *et al.* Seasonal variability of land-ocean groundwater nutrient fluxes from a tropical
848 karstic region (southern Java, Indonesia). *Journal of Hydrology* **565**, 662-671 (2018).
849 98 World Bank. INDONESIA COUNTRY REPORT. THE RISE OF METROPOLITAN REGIONS: TOWARDS
850 INCLUSIVE AND SUSTAINABLE REGIONAL DEVELOPMENT 141 (The World Bank, Jakarta, 2010).
851 99 Haas, A. F. *et al.* Global microbialization of coral reefs. *Nature Microbiology* **1**, 1-7 (2016).
852 100 Cárdenas, A. *et al.* Excess labile carbon promotes the expression of virulence factors in coral reef
853 bacterioplankton. *The ISME journal* **12**, 59-76 (2018).
854 101 Senal, M. I. S. *et al.* Nutrient inputs from submarine groundwater discharge on the Santiago reef
855 flat, Bolinao, Northwestern Philippines. *Marine Pollution Bulletin* **63**, 195-200,
856 doi:<https://doi.org/10.1016/j.marpolbul.2011.05.037> (2011).

857
858